This work was supported by the Applied Molecular Biosciences Unit—UCIBIO, which is financed by national funds from Fundação para a Ciência e Tecnologia (UIDP/04378/2020 and UIDB/04378/2020) and by the AgriFood XXI I&D&I project (NORTE-01-0145-FEDER-000041) cofinanced by European Regional Development Fund (ERDF) through the NORTE 2020 (Programa Operacional Regional do Norte 2014/2020). A.R.F. gratefully acknowledges the junior research position (CEECIND/02268/2017, Individual Call to Scientific Employment Stimulus 2017) granted by FCT/MCTES through national funds, and A.P.T. was supported by the Sara Borrell Research Grant (no. CD018/0123) funded by Instituto de Salud Carlos III and co-financed by the European Development Regional Fund (A Way to Achieve Europe program).

About the Author

Dr. Freitas is a contracted investigator at the Research Unit on Applied Molecular Biosciences (UCIBIO@REQUIMTE) in the Faculty of Pharmacy of the University of Porto, Portugal. She is currently the secretary of the Food- and Water-borne Infections Study Group from the European Society of Clinical Microbiology and Infectious Diseases. Her main research interests are in the molecular epidemiology, genomics, and evolution of antimicrobial-resistant *Enterococcus*.

References

1. Davies RH, Lawes JR, Wales AD. Raw diets for dogs and cats: a review, with particular reference to microbiological hazards. J Small Anim Pract. 2019;60:329–39. https://doi.org/10.1111/jsap.13000
2. van den Bunt G, Top J, Hordijk J, de Greeff SC, Mughini-Gras L, Corander J, et al. Intestinal carriage of ampicillin- and vancomycin-resistant *Enterococcus faecium* in humans, dogs and cats in the Netherlands. J Antimicrob Chemother. 2018;73:607–14. https://doi.org/10.1093/jac/dkx455
3. Wu Y, Fan R, Wang Y, Lei L, Feßler AT, Wang Z, et al. Analysis of combined resistance to oxazolidinones and phenicols among bacteria from dogs fed with raw meat/vegetables and the respective food items. Sci Rep. 2019;9:15500. https://doi.org/10.1038/s41598-019-51918-y
4. Bender JK, Cattoir V, Hegstad K, Sadowy E, Coque TM, Westh H, et al. Update on prevalence and mechanisms of resistance to linezolid, tigecycline and daptomycin in enterococci in Europe: Towards a common nomenclature. Drug Resist Updat. 2018;40:25–39. https://doi.org/10.1016/j.drup.2018.10.002
5. European Committee on Antimicrobial Susceptibility Testing (EUCAST). Breakpoint tables for interpretation of MICs and zone diameters. EUCAST version 10.0; 2020 [cited 2020 Dec 1]. https://www.eucast.org/fileadmin/src/media/PDFs/EUCAST_files/Breakpoint_tables/v_11.0_Breakpoint_Tables.pdf
6. Clinical and Laboratory Standards Institute. Performance standards for antimicrobial susceptibility testing: twenty-eighth informational supplement M100. Annapolis Junction (MD): The Institute; 2018.
7. Freitas AR, Tedim AP, Novais C, Lanza VF, Peixe L. Comparative genomics of global *optrA*-carrying *Enterococcus faecalis* uncovers a common chromosomal hotspot for *optrA* acquisition within a diversity of core and accessory genomes. Microb Genom. 2020;6:e000350. https://doi.org/10.1099/mgen.0.000350
8. Novais C, Tedim AP, Lanza VF, Freitas AR, Silveira E, Escada R, et al. Co-diversification of *Enterococcus faecium* core genomes and PBP5: evidences of *pbp5* horizontal transfer. Front Microbiol. 2016;7:1581. https://doi.org/10.3389/fmicb.2016.01581
9. Raven KE, Reuter S, Gouliouris T, Reynolds R, Russell JE, Brown NM, et al. Genome-based characterization of hospital-adapted *Enterococcus faecalis* lineages. Nat Microbiol. 2016;1:15033. https://doi.org/10.1038/nmicrobiol.2015.33
10. Zou J, Tang Z, Yan J, Liu H, Chen Y, Zhang D, et al. Dissemination of linezolid resistance through sex pheromone plasmid transfer in *Enterococcus faecalis*. Front Microbiol. 2020;11:1185. https://doi.org/10.3389/fmicb.2020.01185

Address for correspondence: Luísa Peixe, UCIBIO, Departamento de Ciências Biológicas, Laboratório de Microbiologia, Faculdade de Farmácia, Universidade do Porto, Rua Jorge de Viterbo Ferreira, n. 228, 4050-313 Porto, Portugal; email: lpeixe@ff.up.pt

Highly Pathogenic Avian Influenza A(H5N8) Virus Clade 2.3.4.4b, Western Siberia, Russia, 2020

Ivan Sobolev, Kirill Sharshov, Nikita Dubovitskiy, Olga Kurskaya, Alexander Alekseev, Sergey Leonov, Yuriy Yushkov, Victor Irza, Andrey Komissarov, Artem Fadeev, Daria Danilenko, Junki Mine, Ryota Tsunekuni, Yuko Uchida, Takehiko Saito, Alexander Shestopalov

Author affiliations: Federal Research Center of Fundamental and Translational Medicine, Novosibirsk, Russia (I. Sobolev, K. Sharshov, N. Dubovitskiy, O. Kurskaya, A. Alekseev, A. Shestopalov); Siberian Federal Scientific Centre of Agro-BioTechnologies, Krasnoobsk, Russia (S. Leonov, Y. Yushkov); Federal Governmental State-Financed Institution Federal Centre for Animal Health, Vladimir, Russia (V. Irza); Smorodintsev Research Institute of Influenza, St. Petersburg,

Russia (A. Komissarov, A. Fadeev, D. Danilenko); Division of Transboundary Animal Disease, National Institute of Animal Health, Tsukuba, Japan (J. Mine, R. Tsunekuni, Y. Uchida, T. Saito)

DOI: https://doi.org/10.3201/eid2708.204969

Two variants of highly pathogenic avian influenza A(H5N8) virus were detected in dead poultry in Western Siberia, Russia, during August and September 2020. One variant was represented by viruses of clade 2.3.4.4b and the other by a novel reassortant between clade 2.3.4.4b and Eurasian low pathogenicity avian influenza viruses circulating in wild birds.

In 1996, the highly pathogenic avian influenza (HPAI) A(H5N1) virus subtype of the A/goose/Guangdong/1/1996 lineage was detected in domestic geese in China (*1*). Since 2014, H5Nx HPAI viruses belonging to clade 2.3.4.4 of A/goose/Guangdong/1/1996 lineage have spread internationally, posing a threat to the health of poultry and wild birds. Viruses of clade 2.3.4.4b have been detected in China (2013) and South Korea (2014); in 2016, reassortant strains between 2.3.4.4b and the Eurasian low pathogenicity avian influenza (LPAI) virus, for polymerase basic protein 2 (PB2), polymerase basic protein 1 (PB1), polymerase acidic gene (PA), nucleoprotein (NP), and matrix gene (M) segments, were reported in China (Qinghai Lake) and Russia (Uvs–Nuur Lake) (*2*). Thereafter, 2.3.4.4b viruses and their reassortant strains have spread worldwide and have been identified in poultry and wild birds in multiple countries (*3*).

In January and February 2020, a novel HPAI H5N8 clade 2.3.4.4b virus was detected in Germany. This virus shares 6 gene segments with the HPAI H5N8 virus in Eurasia, Asia, and Africa and 2 gene segments with LPAI virus A(H3N8), which has recently been detected in wild birds of Russia (*4*). HPAI virus strains closely related to isolates from Germany have also been identified in other countries of Europe, according to GISAID (https://www.gisaid.org). In October 2020, HPAI virus related to the variant from Germany has also been isolated in Japan (*5*) and South Korea (*6*).

Other variants of HPAI H5Nx virus were detected in the fall of 2020. Viruses of genetic group B of clade 2.3.4.4 and subtypes H5N8, H5N5, and H5N1 were found in Russia, Kazakhstan, and a number of countries in Europe (*3*,*7*,*8*). These viruses are genetically related to strains isolated in Egypt during 2017–2019 (*7*) and in Iraq in May 2020 (*8*).

The previous cases of H5 HPAI virus in Russia occurred at the end of 2018. In 2019 and the first half of 2020 H5Nx viruses had not been detected in Russia. In August and September 2020, we collected 58 samples from dead domestic birds on private rural farms in Western Siberia. We characterized 7 strains by using complete genome sequencing, phylogenetic analysis, and intravenous pathogenicity index testing. We identified all 7 strains as HPAI viruses on the basis of the amino acid sequence of the hemagglutinin (HA) proteolytic cleavage site (PLREKRRKR|G) and intravenous pathogenicity index values of 2.92–2.93 in chickens (Table).

We divided the isolated strains into 2 groups according to the sequences of the genome segments. Group 1 consists of 4 strains, whereas group 2 consists of 3 strains (Table). By using BLAST analysis (http://blast.ncbi.nlm.nih.gov/Blast.cgi), we found all 8 genome segments of group 1 and the 3 genome segments (HA, M, and NS) of group 2 to be closely related (99.01%–100% nucleotide identity) to the genome segments of HPAI clade 2.3.4.4b virus strains isolated in Russia, Kazakhstan, and Europe in the summer and fall of 2020. We found the genome segments of neuraminidase, PB2, PB1, PA, and NP in group 2 to be related (98.38%–99.06% nucleotide identity) to different LPAI viruses from Eurasia.

Phylogenetic analysis showed that the whole genome of group 1 and HA, M, and nonstructural gene genome segments of group 2 clustered with HPAI H5N8 clade 2.3.4.4b virus. They were also related to H5N8 viruses from Egypt (2019) and Iraq (May 2020) but were not related to the H5N8 variants from Germany in early 2020 (Figure; Appendix 1 Figures 1–7, https://wwwnc.cdc.gov/EID/article/27/8/20-4969-App1.pdf). The neuraminidase, PB2, PB1, PA, and NP segments of group 2 viruses clustered with

Table. Highly pathogenic avian influenza A viruses subtype H5N8 isolated from birds, Novosibirsk, Western Siberia, Russia, 2020*

Group	Isolate ID	Site	Collection date	IVPI value
1	A/goose/Russia_Novosibirsk region/1-12/2020	Intestine	2020 Sep 15	2.92
1	A/goose/Russia_Omsk region/55-1/2020	Intestine	2020 Aug 29	2.92
1	A/chicken/Russia_Novosibirsk region/1910-1/2020	Liver	2020 Sep 22	2.92
1	A/chicken/Russia_Novosibirsk region/1910-2/2020	Intestine	2020 Sep 22	2.92
2	A/chicken/Russia_Novosibirsk region/3-1/2020	Intestine	2020 Sep 20	2.93
2	A/chicken/Russia_Novosibirsk region/3-15/2020	Intestine	2020 Sep 20	2.93
2	A/chicken/Russia_Novosibirsk region/3-29/2020	Brain	2020 Sep 20	2.93

*ID, identification; IVPI, intravenous pathogenicity index.

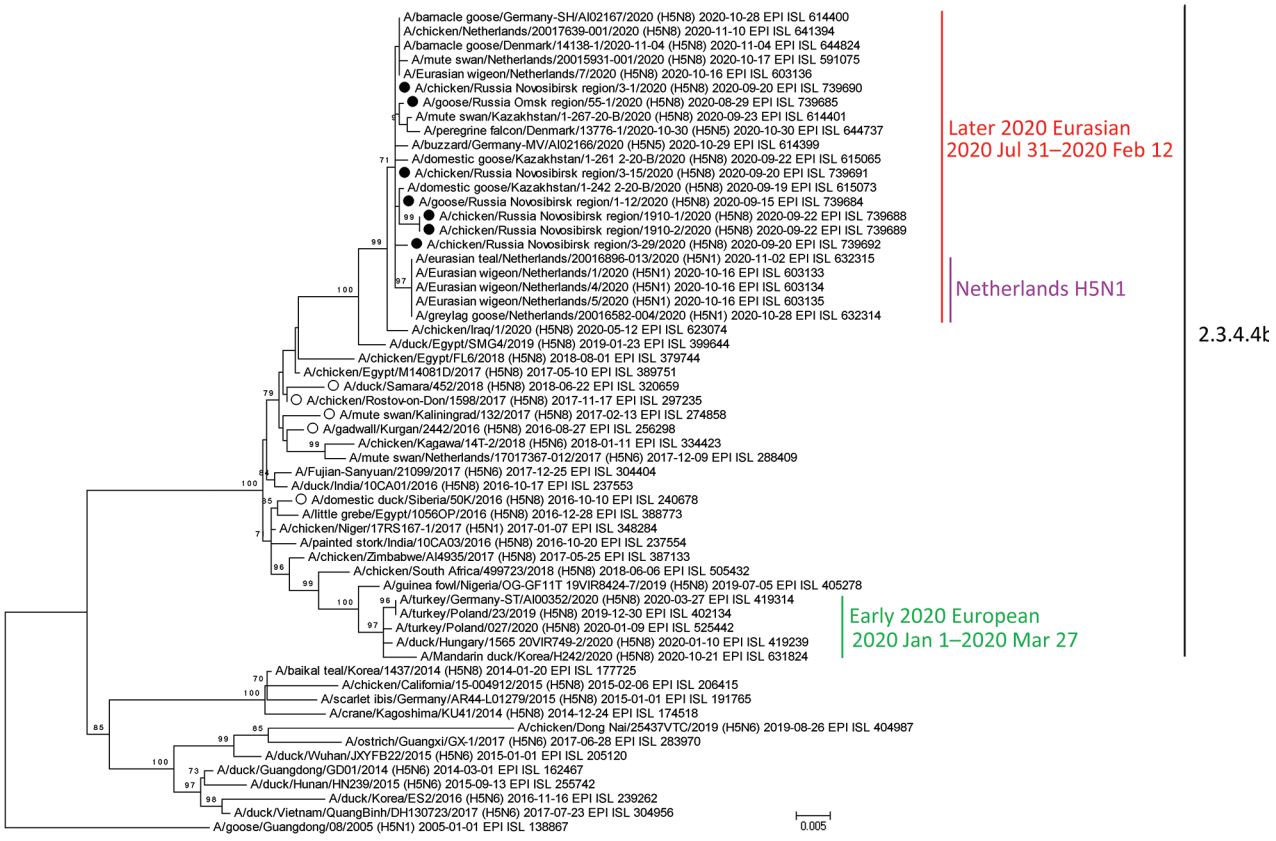

Figure. Maximum-likelihood phylogenetic tree of the hemagglutinin segment of HPAI subtype H5N8 virus isolated from birds, Novosibirsk, Western Siberia, Russia, 2020, and reference segments from GISAID (http://www.gisaid.org). Filled circles indicate HPAI H5N8 virus strains from Russia isolated in 2020; open circles indicate strains from Russia isolated during 2016–2018. Virus identification number, date of identification, and GISAID accession number are provided for all sequences. HPAI, highly pathogenic avian influenza.

LPAI viruses identified in Eurasia. Consequently, group 2 strains are reassortant strains between Egyptian-like HPAI and LPAI viruses from Eurasia (Appendix 1 Figure 8). Of note, PB2, PA, and NP segments of group 2 isolates clustered on phylogenetic trees (nucleotide identity of 97.32%–97.45% for PB2, 98.98%–99.02% for PA, and 98.86%–99.00% for NP) with the HPAI H5N1 reassortants isolated in the fall of 2020 in the Netherlands (*8*). PB1 segments showed a lower level of identity (96.21%–96.26%).

On the basis of our phylogenetic data, chronology of virus isolations, general birds' flyways, and previously described patterns of HPAI viruses spreading from Siberia during 2005–2006, 2014, and 2016–2017 (*3*,*9*,*10*), we suggest that new H5N8 viral strain from Eurasia in late 2020 possibly descended from the H5N8 virus circulating in Egypt during 2017–2019 and then disseminated through Iraq into Western Siberia and North Kazakhstan during the spring migration. Egyptian-like HPAI H5N8 virus possibly reached breeding and staging areas in Siberia in early 2020, spread in wild bird populations, and reassorted with LPAI viruses. During fall migration, standard Egyptian-like HPAI H5N8 virus and novel reassortant strains spread to the European part of Eurasia, leading to a reassortment event, which has been detected in Netherlands. However, further studies of 2020–2021 European H5Nx viruses are needed to verify this hypothesis.

Acknowledgments

We are grateful to GISAID's EpiFlu Database (http://www.gisaid.org) and to the authors who provided sequence information (Appendix 2, https://wwwnc.cdc.gov/EID/article/27/8/20-4969-App2.xlsx).

Laboratory diagnostics, virologic experiments, and analysis in this study was supported by the Russian Science Foundation (project no. RSF 20-44-07001), and sample collection was supported by the Russian Foundation for Basic Research (project no. RFBR 19-54-55004). This study was also supported partly by the Ministry of Agriculture,

Forestry and Fisheries of Japan (project no. JPJ008837) as part of its program for funding commissioned projects for promotion of strategic international collaborative research.

About the Author

Dr. Sobolev is a researcher at the Federal Research Center of Fundamental and Translational Medicine, Russia. His primary research interest is the molecular diagnosis and epidemiology of avian influenza viruses.

References

1. Duan L, Campitelli L, Fan XH, Leung YH, Vijaykrishna D, Zhang JX, et al. Characterization of low-pathogenic H5 subtype influenza viruses from Eurasia: implications for the origin of highly pathogenic H5N1 viruses. J Virol. 2007;81:7529–39. https://doi.org/10.1128/JVI.00327-07
2. Lee DH, Sharshov K, Swayne DE, Kurskaya O, Sobolev I, Kabilov M, et al. Novel reassortant clade 2.3.4.4 avian influenza A(H5N8) virus in wild aquatic birds, Russia, 2016. Emerg Infect Dis. 2017;23:359–60. https://doi.org/10.3201/eid2302.161252
3. Verhagen JH, Fouchier RAM, Lewis N. Highly pathogenic avian influenza viruses at the wild-domestic bird interface in Europe: future directions for research and surveillance. Viruses. 2021;13:212. https://doi.org/10.3390/v13020212
4. King J, Schulze C, Engelhardt A, Hlinak A, Lennermann SL, Rigbers K, et al. Novel HPAIV H5N8 reassortant (clade 2.3.4.4b) detected in Germany. Viruses. 2020;12:281. https://doi.org/10.3390/v12030281
5. Isoda N, Twabela AT, Bazarragchaa E, Ogasawara K, Hayashi H, Wang ZJ, et al. Re-invasion of H5N8 high pathogenicity avian influenza virus clade 2.3.4.4b in Hokkaido, Japan, 2020. Viruses. 2020;12:1439. https://doi.org/10.3390/v12121439
6. Jeong S, Lee DH, Kwon JH, Kim YJ, Lee SH, Cho AY, et al. Highly pathogenic avian influenza clade 2.3.4.4b subtype H5N8 virus isolated from Mandarin Duck in South Korea, 2020. Viruses. 2020;12:1389. https://doi.org/10.3390/v12121389
7. Beerens N, Heutink R, Harders F, Roose M, Pritz-Verschuren S, Germeraad E, et al. Novel incursion of a highly pathogenic avian influenza subtype H5N8 virus in the Netherlands, October 2020. Emerg Infect Dis. 2021;27:1750–3. https://doi.org/10.3201/eid2706.204464
8. Lewis NS, Banyard AC, Whittard E, Karibayev T, Al Kafagi T, Chvala I, et al. Emergence and spread of novel H5N8, H5N5 and H5N1 clade 2.3.4.4 highly pathogenic avian influenza in 2020. Emerg Microbes Infect. 2021;10:148–51. https://doi.org/10.1080/22221751.2021.1872355
9. Olsen B, Munster VJ, Wallensten A, Waldenström J, Osterhaus AD, Fouchier RA. Global patterns of influenza a virus in wild birds. Science. 2006;312:384–8. https://doi.org/10.1126/science.1122438
10. Marchenko V, Goncharova N, Susloparov I, Kolosova N, Gudymo A, Svyatchenko S, et al. Isolation and characterization of H5Nx highly pathogenic avian influenza viruses of clade 2.3.4.4 in Russia. Virology. 2018;525:216–23. https://doi.org/10.1016/j.virol.2018.09.024

Address for correspondence: Ivan Sobolev, Federal Research Center of Fundamental and Translational Medicine, Timakov st. 2, Novosibirsk, 630117, Russia; email: sobolev_i@hotmail.com

Tuberculosis-Associated Hospitalizations and Deaths after COVID-19 Shelter-In-Place, San Francisco, California, USA

Janice K. Louie, Rocio Agraz-Lara, Laura Romo, Felix Crespin, Lisa Chen,[1] Susannah Graves[1]

Author affiliations: San Francisco Department of Public Health Tuberculosis Prevention and Control Program, San Francisco, California, USA (J.K. Louie, R. Agraz-Lara, L. Romo, F. Crespin, S. Graves); University of California, San Francisco (J.K. Louie, L. Chen)

DOI: https://doi.org/10.3201/eid2708.210670

A mandated shelter-in-place and other restrictions associated with the coronavirus disease pandemic precipitated a decline in tuberculosis diagnoses in San Francisco, California, USA. Several months into the pandemic, severe illness resulting in hospitalization or death increased compared with prepandemic levels, warranting heightened vigilance for tuberculosis in at-risk populations.

Since the emergence of a novel coronavirus, severe acute respiratory syndrome coronavirus 2 (SARS-CoV-2), which causes coronavirus disease (COVID-19), unprecedented measures have been recommended to reduce transmission. In San Francisco, California, USA, progressively restrictive health officer orders implemented since early 2020 have included travel quarantines, shelter-in-place (SIP), deferral of routine medical appointments and elective surgeries, closure of public-facing events and businesses, and isolation and quarantine when appropriate (*1*). Nationwide, disruptions in medical services have contributed to delaying or avoiding routine care and a decrease in non–COVID-19-related hospital admissions and emergency department visits (*2*). Similarly, worldwide tuberculosis (TB) case reports have declined, including in San Francisco, where a ≈60% decrease in newly diagnosed TB cases compared with prior years was observed in the first 4 months of the pandemic (*3*,*4*).

The San Francisco Department of Public Health (SFDPH) Tuberculosis Prevention and Control Program manages all cases of active TB in San Francisco residents (≈881,549 population). In 2019, San Francisco had a high incidence of TB, with rates >4-fold higher (11.9 cases/100,000 persons) than the national rate. The affected population is predominantly

[1]These senior authors contributed equally to this article.

Article DOI: https://doi.org/10.3201/eid2708.204969

Highly Pathogenic Avian Influenza A(H5N8) Virus Clade 2.3.4.4b, Western Siberia, Russia, 2020

Appendix 1

Materials and Methods

Samples

We collected 58 samples from dead domestic birds (chickens and geese) from small, private, village farms in Western Siberia between August and September 2020. In 30 of these samples, influenza virus H5 subtype were detected using real-time polymerase chain reaction (AmpliSens Influenza virus A H5N1-FRT PCR kit, AmpliSens, Russia). A total of 15 isolates of H5 viruses were isolated from 10-day-old chicken embryonating eggs using chicken embryo inoculation. All viruses caused the death of chicken embryos within two days. Samples and isolates were demonstrated to be H5 positive using real-time PCR.

It should be noted that samples were collected from small, private, rural farms, which have several of the following features. First, they allow for free grazing of poultry; ducks and geese can visit water bodies, such as lakes, near the village. Second, small, private, rural farms lack any biosafety measures. Third, birds of different species often cohabit the farm, which ensures transmission of the virus to chickens from geese or ducks that visit the lake and interact with wild birds there.

Therefore, they are convenient points for HPAIVs surveillance. However, owing to the lack of control over the activities of such small farms, it is difficult to clearly understand the causes and parameters of viral transmission on such farms. We assume that the reason is complex; poultry on free grazing farms interact with wild birds, and the lack of biosafety measures and the residence of several species of birds in a limited area of the farm promotes the spread of viruses across populations and species.

The selection of seven isolates for the further study was based on the “one farm – one isolate” principle. Isolates with the same collection date (A/chicken/Russia_Novosibirsk region/3-1/2020, A/chicken/Russia_Novosibirsk region/3-15/2020 and A/chicken/Russia_Novosibirsk region/3-29/2020 – 20.09.2020; A/chicken/Russia_Novosibirsk region/1910-1/2020 and A/chicken/Russia_Novosibirsk region/1910-2/2020 – 22.09.2020) were collected from different farms but in one village.

Genome sequencing and phylogenetic analysis

Complete genome sequencing of 7 influenza H5N8 isolates was performed by nanopore sequencing technology (Oxford-Nanopore MinION). RNA from was extracted using QIAamp Viral RNA Mini Kit. Whole-genome amplification of Influenza A virus genome was performed using protocol by Zhou et al. (*1*) Primers were modified by adding ONT universal tags: 5′-TTTCTGTTGGTGCTGATATTGC-3′ and 5′-ACTTGCCTGTCGCTCTATCTTC-3′ for forward and reverse primers, respectively. 1D Ligation sequencing kit (SQK-LSK109) with PCR barcoding expansion (EXP-PBC096) was utilized for sequencing library preparation. MinION (Oxford Nanopore) (flow cell R9.4.1) was used for whole-genome sequencing. Fast5 files produced by minION were basecalled and demultiplexed using guppy v3.6.0. Reads were mapped onto the reference sequence using minimap2 v2.17 with default settings. SAMtools-mpileup v1.10 was used to produce consensus sequences.

Nucleotide sequences were deposited in the GISAID database under accession number EPI_ISL_739684-EPI_ISL_739692. Phylogenetic trees were reconstructed using sequences of H5N8 influenza viruses isolated worldwide since 2016 from BLAST (GISAID). Initial Maximum-likelihood phylogenies for each of the gene segments were generated with RAxML (*2*) using the general time-reversible nucleotide substitution model. Final dendrograms were generated and visualized with MEGA5 (*3*). Bootstrap support values were generated using 1,000 rapid bootstrap replicates.

Migration studies

We considered the map (*4*) of the generalized waterbirds’ flyways (Wetlands International group) and performed large-scale analysis of movements of waterbirds in Southwest Siberian. Locations of virus isolations on a map for waterbird migration (Wader Flyways), according to the Wetlands International group suggests, that the most likely way of

Egyptian-like virus spread with waterbird spring migration might be along the Asian–East African or/and Mediterranean/Black Sea flyways. This was verified by large-scale analysis of ring recoveries from waterbirds in Eurasia (*4*).

Intravenous pathogenicity index (IVPI)

All animal experiments were approved by the Ethics Committee of the Federal Research Centre of Fundamental and Translational Medicine (Ethics Committee decision Nº36/1, 19.11.2020). For the determination of IVPI of 9 viruses, 0.1 ml of 1:10 dilution of infectious allantoic fluids were inoculated intravenously into ten 6-week-old specific pathogen free chickens. The IVPI was calculated according to the OIE standard protocol (available at: http://www.oie.int/international-standard-setting/terrestrial-code/). Isolates with an IVPI > 1.2 were determined to be HPAIV. The challenge study and all experiments with live viruses were conducted in a biosafety level 3 facility.

References

1. Zhou B, Donnelly ME, Scholes DT, St George K, Hatta M, Kawaoka Y, et al. Single-reaction genomic amplification accelerates sequencing and vaccine production for classical and swine origin human influenza a viruses. J Virol. 2009;83:10309–13. PubMed https://doi.org/10.1128/JVI.01109-09

2. Stamatakis A. RAxML version 8: a tool for phylogenetic analysis and post-analysis of large phylogenies. Bioinformatics. 2014;30:1312–3. PubMed https://doi.org/10.1093/bioinformatics/btu033

3. Tamura K, Peterson D, Peterson N, Stecher G, Nei M, Kumar S. MEGA5: molecular evolutionary genetics analysis using maximum likelihood, evolutionary distance, and maximum parsimony methods. Mol Biol Evol. 2011;28:2731–9. PubMed https://doi.org/10.1093/molbev/msr121

4. Veen J, Yurlov AK, Delany SN, Mihantiev AI, Selivanova MA, Boere GC. An atlas of movements of Southwest Siberian waterbirds. Wageningen (Netherlands): Wetlands International; 2005.

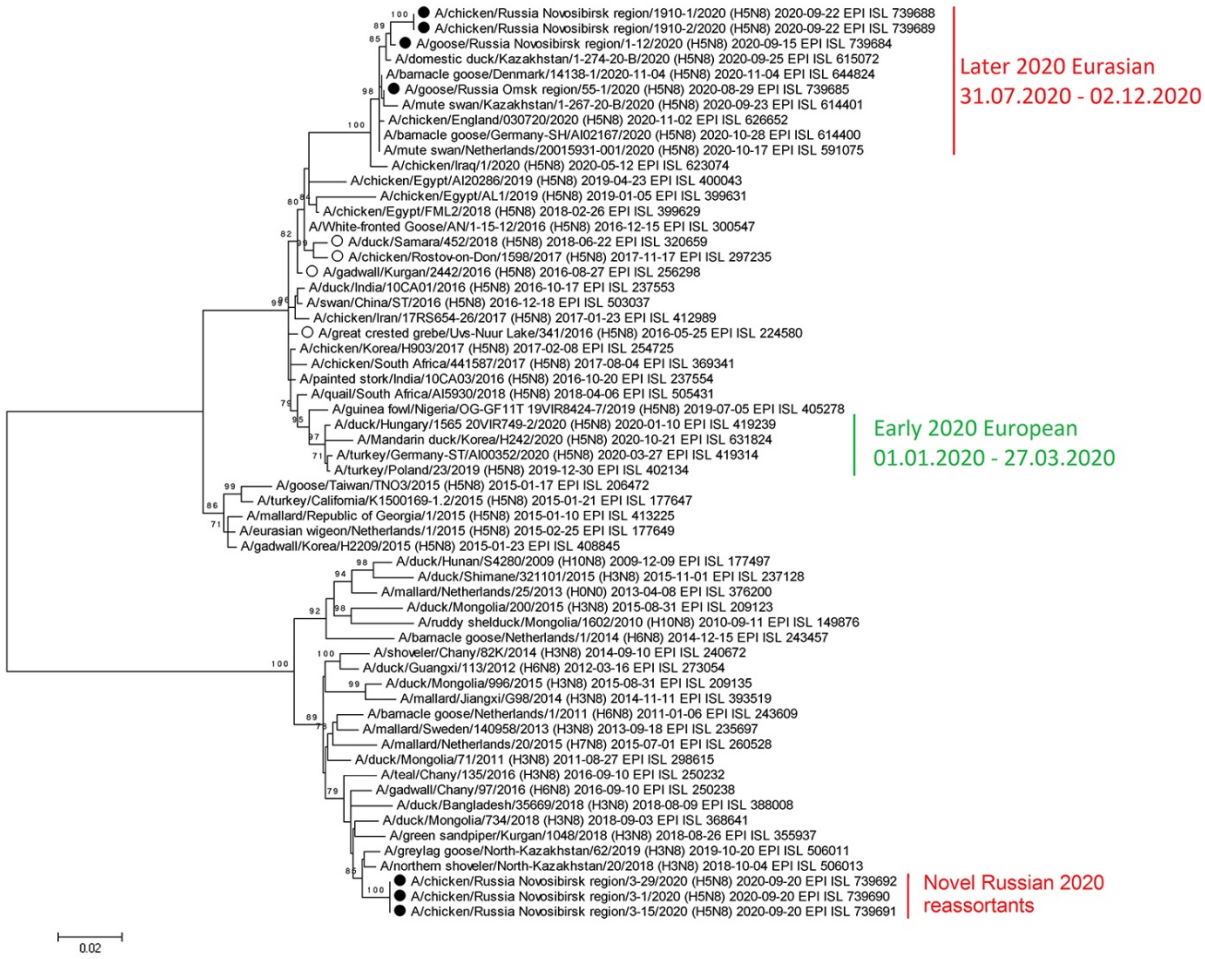

Appendix 1 Figure 1. Maximum-likelihood phylogenetic tree of the NA segment. Black circles - HPAIVs H5N8 from Russia isolated in 2020. White circles - Russian HPAIVs H5N8 isolated in 2016-2018.

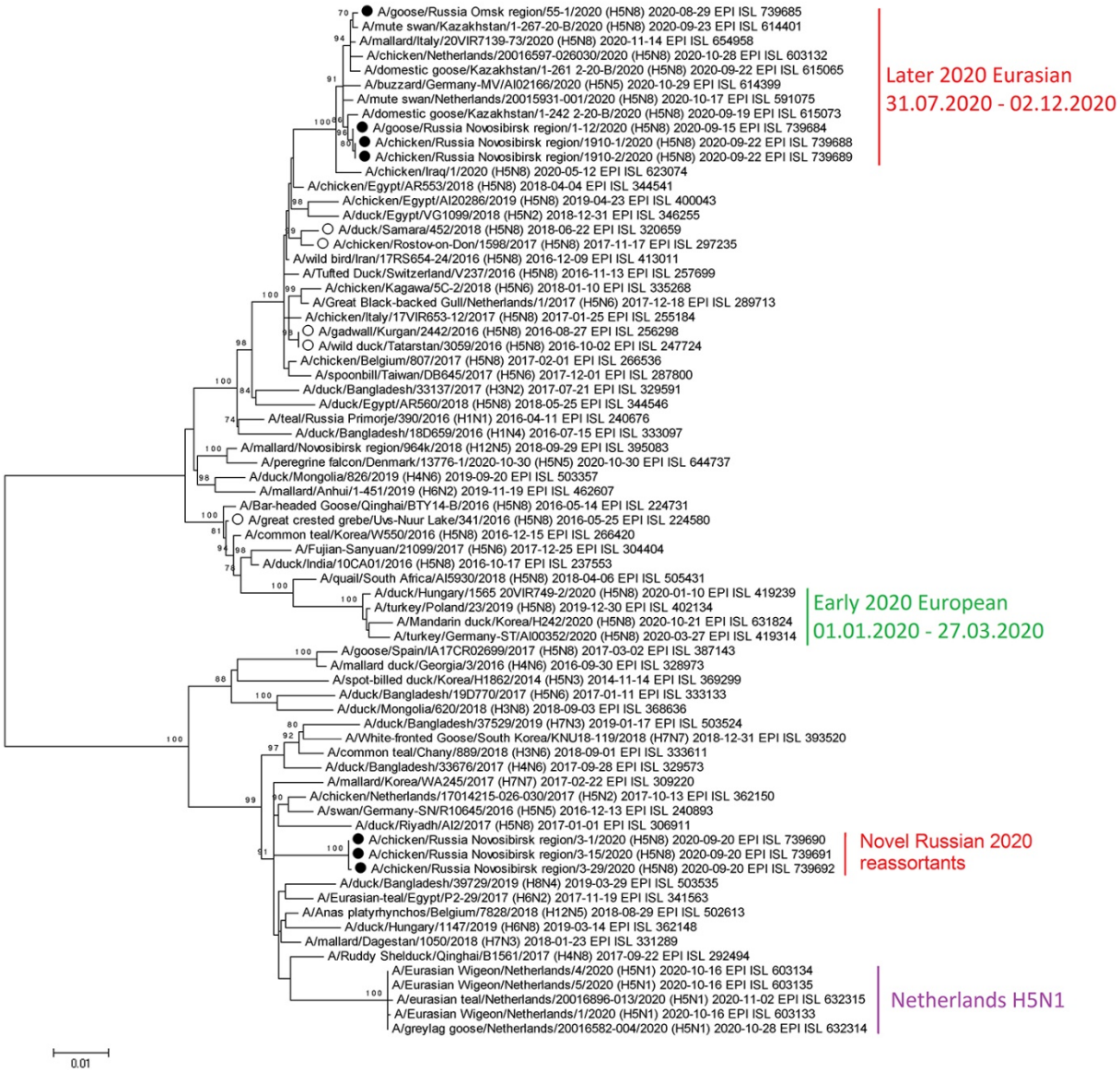

Appendix 1 Figure 2. Maximum-likelihood phylogenetic tree of the PB2 segment. Black circles - HPAIVs H5N8 from Russia isolated in 2020. White circles - Russian HPAIVs H5N8 isolated in 2016-2018.

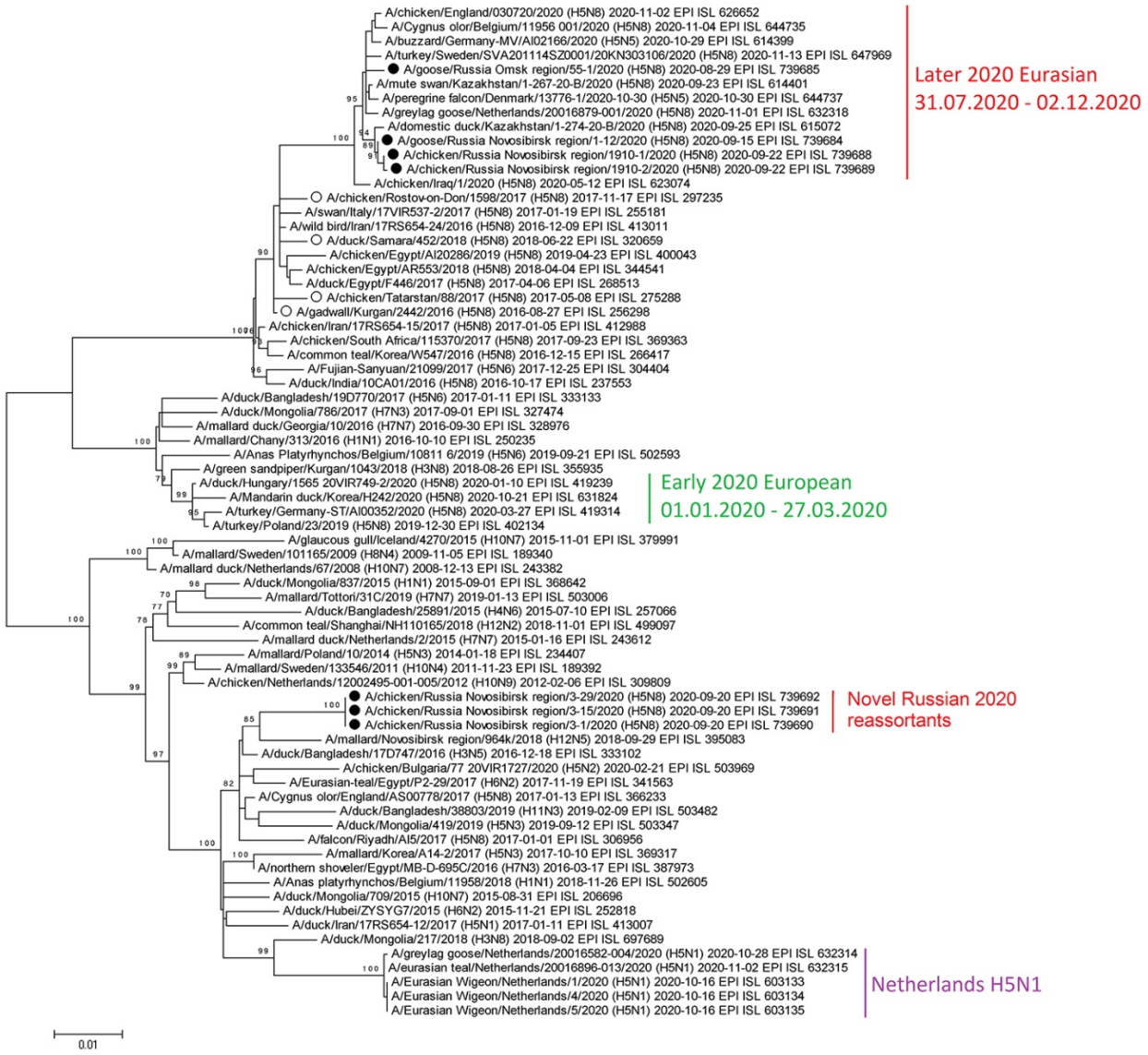

Appendix 1 Figure 3. Maximum-likelihood phylogenetic tree of the PB1 segment. Black circles - HPAIVs H5N8 from Russia isolated in 2020. White circles - Russian HPAIVs H5N8 isolated in 2016-2018.

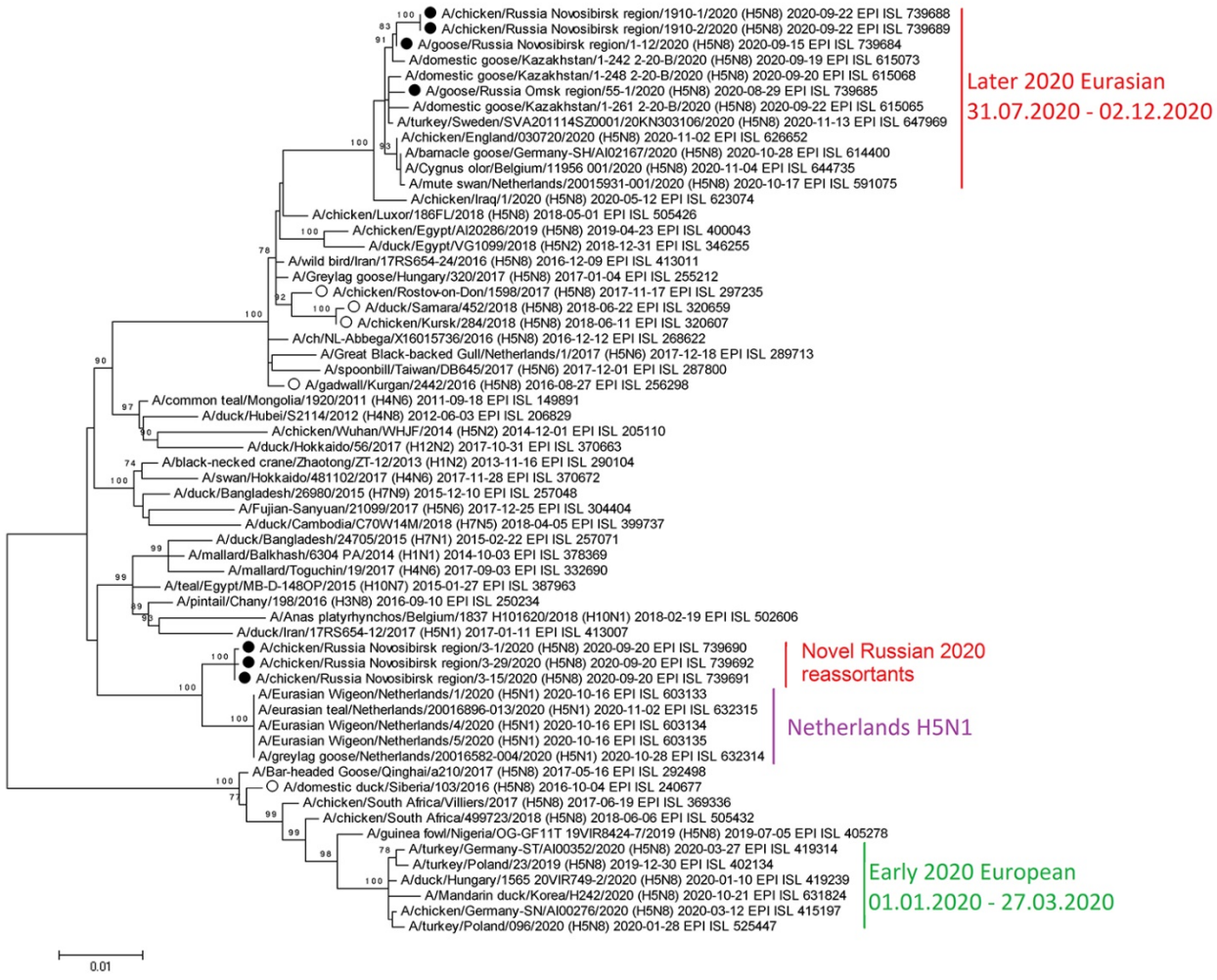

Appendix 1 Figure 4. Maximum-likelihood phylogenetic tree of the PA segment. Black circles - HPAIVs H5N8 from Russia isolated in 2020. White circles - Russian HPAIVs H5N8 isolated in 2016-2018.

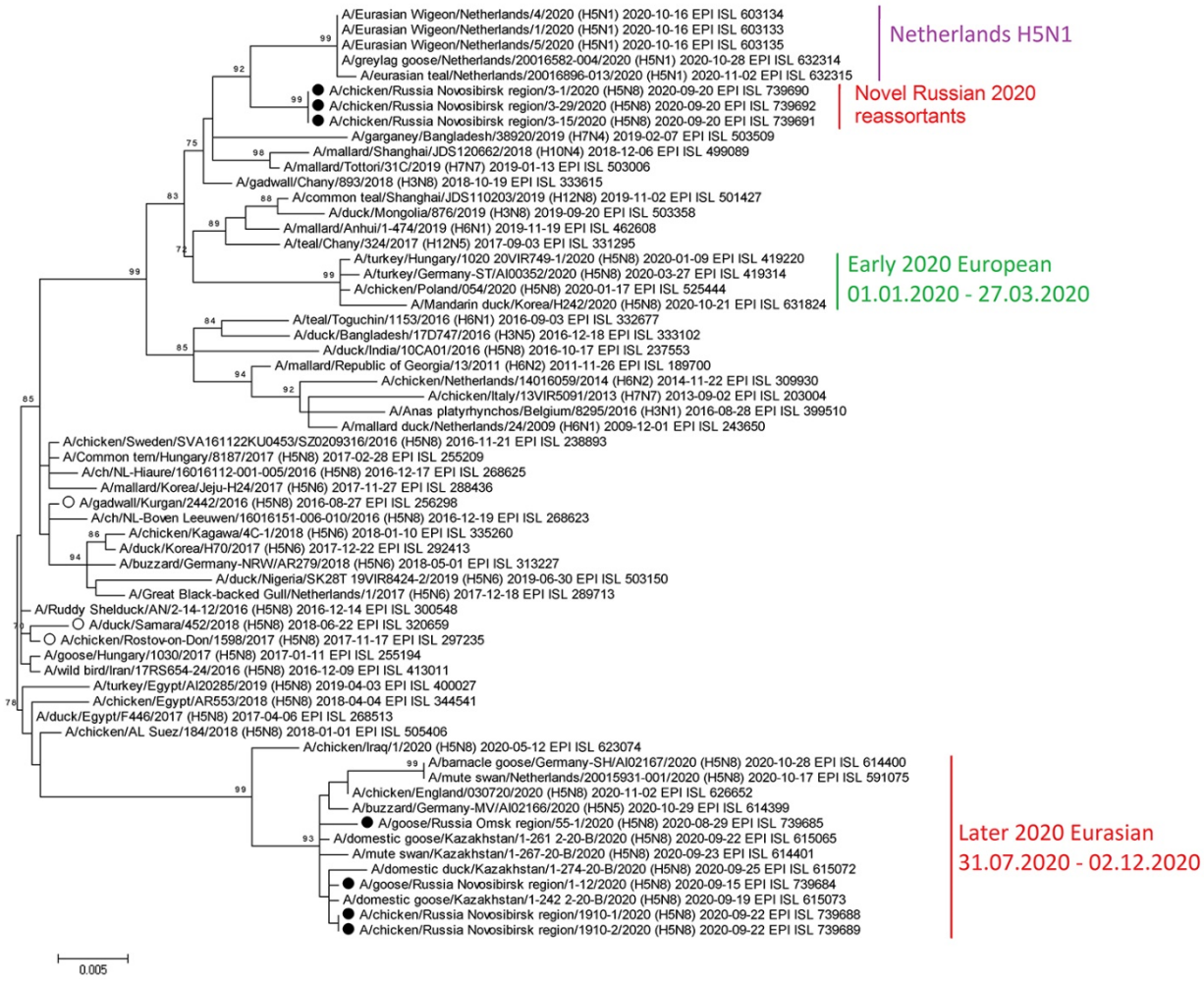

Appendix 1 Figure 5. Maximum-likelihood phylogenetic tree of the NP segment. Black circles - HPAIVs H5N8 from Russia isolated in 2020. White circles - Russian HPAIVs H5N8 isolated in 2016-2018.

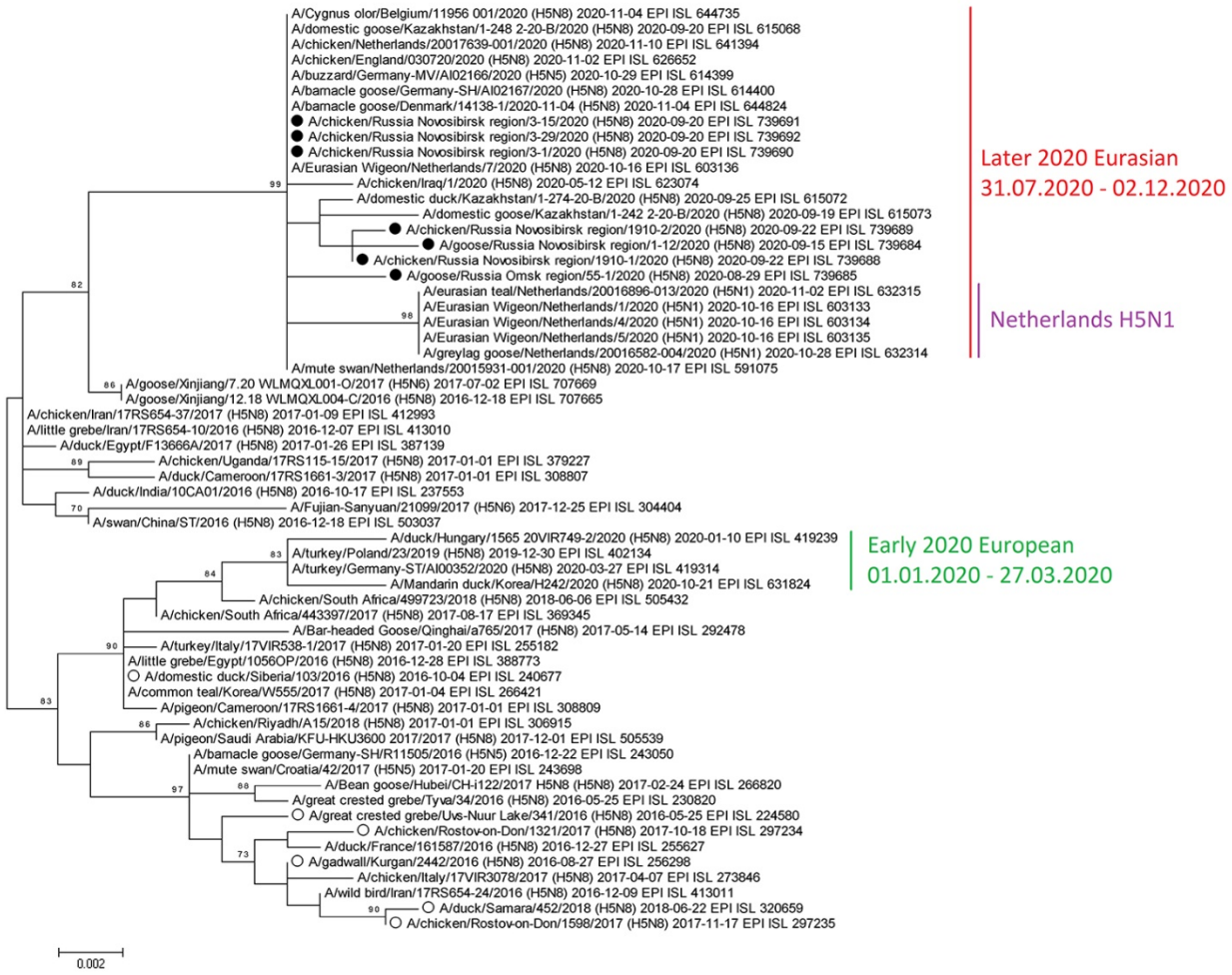

Appendix 1 Figure 6. Maximum-likelihood phylogenetic tree of the MP segment. Black circles - HPAIVs H5N8 from Russia isolated in 2020. White circles - Russian HPAIVs H5N8 isolated in 2016-2018.

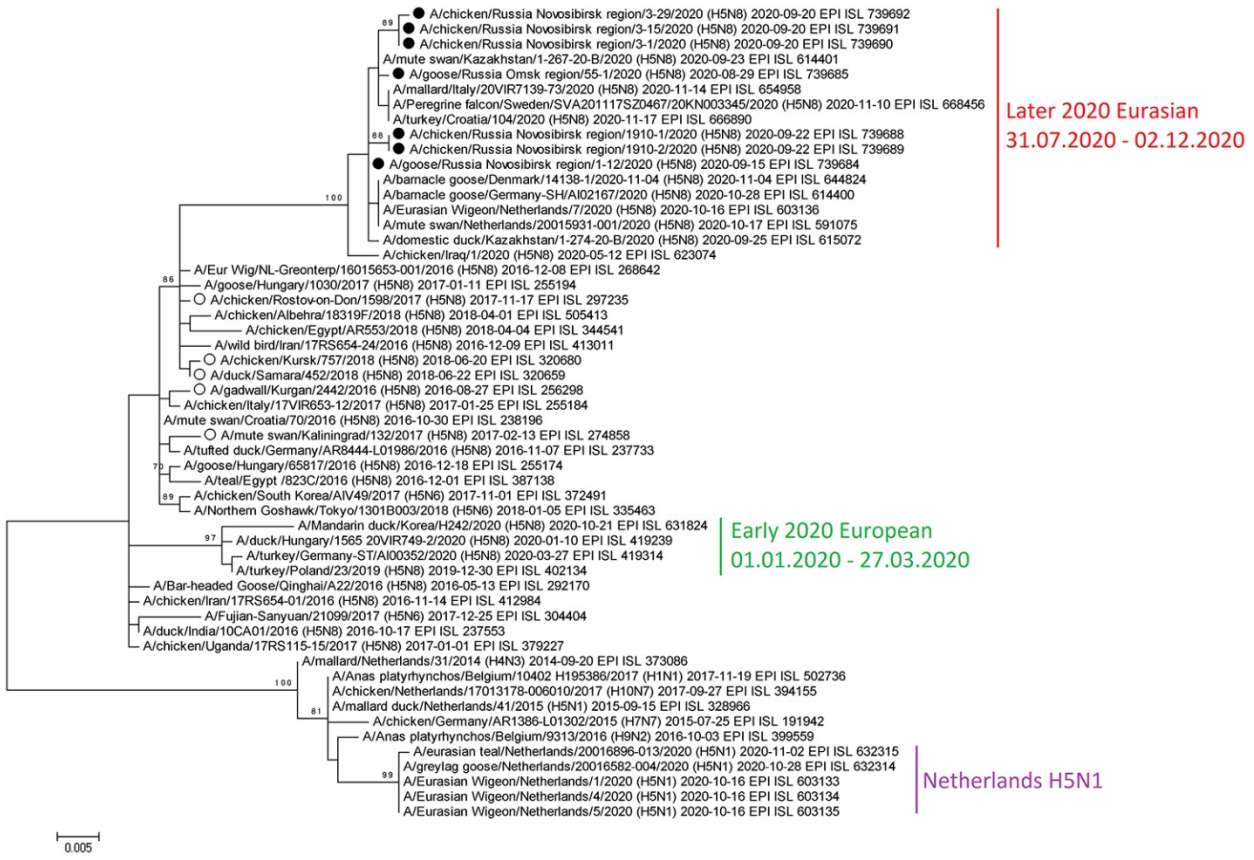

Appendix 1 Figure 7. Maximum-likelihood phylogenetic tree of the NS segment. Black circles - HPAIVs H5N8 from Russia isolated in 2020. White circles - Russian HPAIVs H5N8 isolated in 2016-2018.

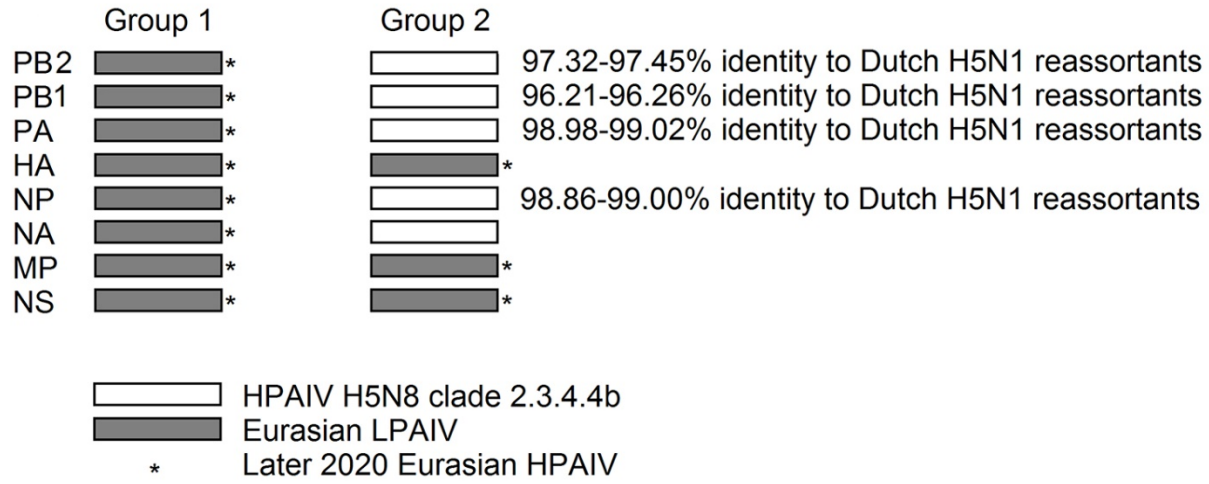

Appendix 1 Figure 8. Differences of the genome segments composition between isolates of groups 1 and 2. The percentage of identity to Dutch H5N1 reassortants is based on matrices of pairwise distances between Russian and Dutch strains (Appendix 1 Figure 10).

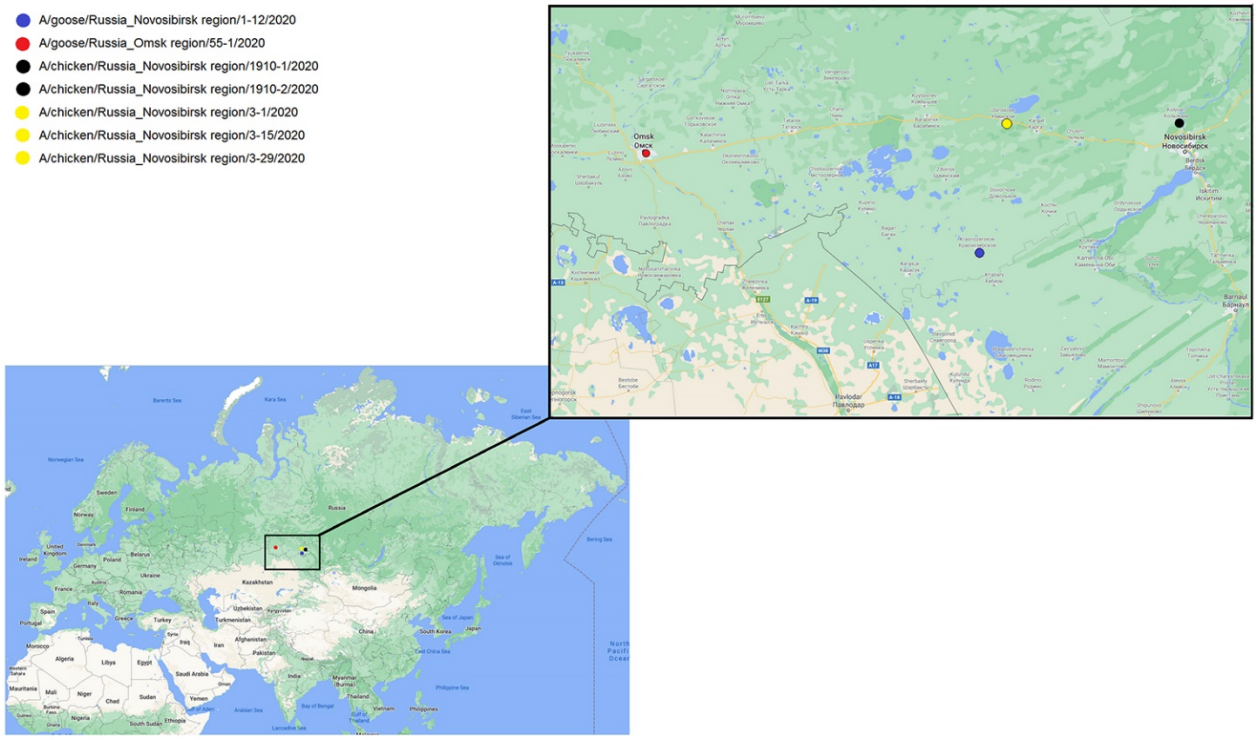

Appendix 1 Figure 9. Sampling locations. Map was retrieved from Google Maps (https://www.google.com/maps).

PB2							
A/chicken/Russia_Novosibirsk_region/3-1/2020							
A/chicken/Russia_Novosibirsk_region/3-29/2020	99,96						
A/chicken/Russia_Novosibirsk_region/3-15/2020	100,00	99,96					
A/Eurasian_Wigeon/Netherlands/1/2020	97,36	97,41	97,36				
A/Eurasian_Wigeon/Netherlands/4/2020	97,41	97,45	97,41	99,96			
A/Eurasian_Wigeon/Netherlands/5/2020	97,41	97,45	97,41	99,96	100,00		
A/greylag_goose/Netherlands/20016582-004/2020	97,41	97,45	97,41	99,96	100,00	100,00	
A/eurasian_teal/Netherlands/20016896-013/2020	97,32	97,36	97,32	99,87	99,91	99,91	99,91
PB1							
A/chicken/Russia_Novosibirsk_region/3-1/2020							
A/chicken/Russia_Novosibirsk_region/3-29/2020	100,00						
A/chicken/Russia_Novosibirsk_region/3-15/2020	100,00	100,00					
A/Eurasian_Wigeon/Netherlands/1/2020	96,21	96,21	96,21				
A/Eurasian_Wigeon/Netherlands/4/2020	96,21	96,21	96,21	100,00			
A/Eurasian_Wigeon/Netherlands/5/2020	96,21	96,21	96,21	100,00	100,00		
A/greylag_goose/Netherlands/20016582-004/2020	96,21	96,21	96,21	99,91	99,91	99,91	
A/eurasian_teal/Netherlands/20016896-013/2020	96,26	96,26	96,26	99,96	99,96	99,96	99,96
PA							
A/chicken/Russia_Novosibirsk_region/3-1/2020							
A/chicken/Russia_Novosibirsk_region/3-29/2020	99,91						
A/chicken/Russia_Novosibirsk_region/3-15/2020	99,95	99,95					
A/Eurasian_Wigeon/Netherlands/1/2020	98,98	98,98	99,02				
A/Eurasian_Wigeon/Netherlands/4/2020	98,98	98,98	99,02	100,00			
A/Eurasian_Wigeon/Netherlands/5/2020	98,98	98,98	99,02	100,00	100,00		
A/greylag_goose/Netherlands/20016582-004/2020	98,98	98,98	99,02	100,00	100,00	100,00	
A/eurasian_teal/Netherlands/20016896-013/2020	98,98	98,98	99,02	100,00	100,00	100,00	100,00
NP							
A/chicken/Russia_Novosibirsk_region/3-1/2020							
A/chicken/Russia_Novosibirsk_region/3-15/2020	100,00						
A/chicken/Russia_Novosibirsk_region/3-29/2020	100,00	100,00					
A/Eurasian_Wigeon/Netherlands/1/2020	99,00	99,00	99,00				
A/Eurasian_Wigeon/Netherlands/4/2020	99,00	99,00	99,00	100,00			
A/Eurasian_Wigeon/Netherlands/5/2020	99,00	99,00	99,00	100,00	100,00		
A/greylag_goose/Netherlands/20016582-004/2020	99,00	99,00	99,00	100,00	100,00	100,00	
A/eurasian_teal/Netherlands/20016896-013/2020	98,86	98,86	98,86	99,87	99,87	99,87	99,87

Appendix 1 Figure 10. Matrices of pairwise distances between Russian and Dutch strains.